

Choice Outweighs Effort: Facilitating Complementary Knowledge Fusion in Federated Learning via Re-calibration and Merit-discrimination

Ming Yang^{a,b}, Dongrun Li^{a,b}, Xin Wang^{a,b,*}, Xiaoyang Yu^{a,b}, Xiaoming Wu^{a,b} and Shibo He^c

^aKey Lab. of Computing Power Network and Information Security, Ministry of Education, Shandong Computer Science Center, Qilu University of Technology (Shandong Academy of Sciences), Jinan, China

^bShandong Provincial Key Lab. of Industrial Network and Information System Security, Shandong Fundamental Research Center for Computer Science, Jinan, China

^cCollege of Control Science and Engineering, Zhejiang University, Hangzhou, China

Abstract. Cross-client data heterogeneity in federated learning induces biases that impede unbiased consensus condensation and the complementary fusion of generalization- and personalization-oriented knowledge. While existing approaches mitigate heterogeneity through model decoupling and representation center loss, they often rely on static and restricted metrics to evaluate local knowledge and adopt global alignment too rigidly, leading to consensus distortion and diminished model adaptability. To address these limitations, we propose *FedMate*¹, a method that implements bilateral optimization: On the server side, we construct a dynamic global prototype, with aggregation weights calibrated by holistic integration of sample size, current parameters, and future prediction; a category-wise classifier is then fine-tuned using this prototype to preserve global consistency. On the client side, we introduce complementary classification fusion to enable merit-based discrimination training and incorporate cost-aware feature transmission to balance model performance and communication efficiency. Experiments on five datasets of varying complexity demonstrate that *FedMate* outperforms state-of-the-art methods in harmonizing generalization and adaptation. Additionally, semantic segmentation experiments on autonomous driving datasets validate the method’s real-world scalability.

Keywords: Personalized Federated Learning, Heterogeneous Data, Complementary Knowledge Fusion

1 Introduction

During artificial intelligence (AI) model training, participants often seek to enhance their models by leveraging others’ data while unwilling to share their own private and high-value information [23]. Federated learning (FL) addresses this dilemma by facilitating the exchange of locally trained models instead of raw data [25], thereby enabling secure knowledge sharing and collaborative training across distributed clients. A streamlined implementation framework allows FL to be seamlessly applied to lightweight models [30]. Recent work, such as Google’s DiLoCo framework [3], demonstrates the scalability of FL for large language models, reinforcing its effectiveness in distributed training. Similarly, frameworks integrating

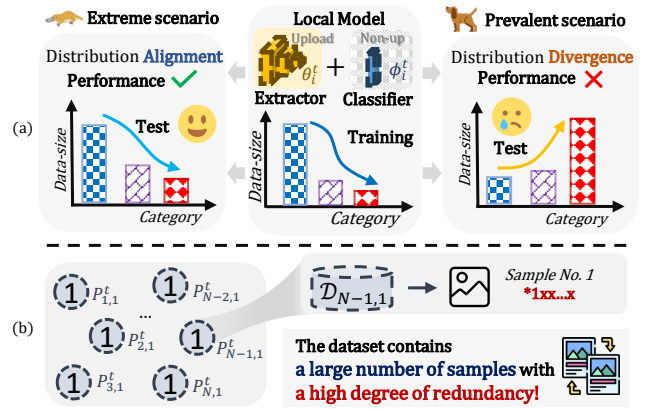


Figure 1. Illustration of the deficiencies in existing FL approaches regarding model decoupling and class center loss design.

general-purpose and specialized models align naturally with FL principles [5, 40], underscoring FL’s versatility.

However, in real-world applications, the decentralized nature of FL data exacerbates cross-client data heterogeneity, hindering the single global model’s ability to adapt to diverse local tasks [39]. Consequently, achieving an effective balance between model generalization and personalization has emerged as a key research challenge. To address this, personalized federated learning (PFL) has been introduced, aiming to optimize this trade-off through fine-grained methodologies [7, 28, 4, 38]. PFL typically involves two components: personalized aggregation on the server and personalized training on the client. The latter often proves more effective due to greater resource availability and operational flexibility, enabling closer alignment with the desired objectives. We argue that high-quality local training hinges critically on two factors: selecting personalized modules within the local model and designing both the method and intensity of generalization constraints [42, 12]. Decoupling a model into a shared feature extractor and a task-specific classifier provides a promising approach to modular personalization in PFL [1, 7]. This architecture leverages the transferable nature of feature representations: a globally aggregated feature ex-

* Corresponding author. Email: xinwang@qilu.edu.cn.

¹ Code: <https://github.com/Dongrun-Li/FedMate.git>.

tractor (e.g., via FedAvg [25]) can effectively capture generalizable features across clients, even under data distribution shifts. In contrast, classifiers—being more sensitive to local task distributions—typically require personalization to adapt to client-specific variations. However, current methods adopt an extreme dichotomy in optimization: they enforce rigid generalization on the feature extractor while allowing unconstrained personalization of classifiers. This strict decoupling harms component compatibility, ultimately degrading overall model performance. As illustrated in Fig. 1(a), fully personalized classifiers are prone to overfitting, developing biased decision boundaries that limit their operational scope. These limitations arise from: insufficient global knowledge integration during local training, and the lack of a granular trade-off mechanism within each decoupled component. Thus, the core challenge is: *How can decoupled components dynamically incorporate complementary generalization-personalization knowledge during training?*

Leveraging high-quality global knowledge at the feature level enhances generalization by promoting consistent and transferable feature representations across distributed clients. Among existing methods to achieve this, center loss has demonstrated strong potential for improving feature discriminability by enforcing intra-class compactness and inter-class separability [34, 13, 24]. In typical implementations, global representation anchors are employed to impose center loss constraints on local features prior to logits-related cross-entropy optimization. Nevertheless, existing approaches often overlook a critical prerequisite: validating the reliability of these global anchors before initiating global-guided training. Furthermore, during server-side model aggregation, current methods primarily rely on local sample size as a proxy for assessing client update quality. As shown in Fig. 1(b), this simplistic metric proves inadequate for ensuring robust global consensus. This reveals the second fundamental challenge: *How can the server evaluate client updates fairly during aggregation to derive an unbiased global consensus?*

Building upon these two challenges, our key contributions are:

- We propose FedMate, a novel PFL framework that strengthens global guidance through aggregation re-calibration to ensure unbiased consensus, while mutually refining supervisory signals to maintain consistency. Simultaneously, FedMate incorporates discriminative local selection, preserving complementary knowledge between generalization and personalization objectives.
- We implement bilateral optimization on both server and client sides. On the server side, multi-view prototype scrutiny (MPS) and fine-grained category-wise classifier integration (CCI) are employed to ensure robust global aggregation. On the client side, we introduce complementary classification fusion (CCF) to reconcile global coherence and local adaptability, and cost-aware feature transmission (CFT) to regulate communication overhead.
- Through extensive experiments conducted across multiple heterogeneous scenarios and diverse classification datasets, we demonstrate FedMate’s consistent effectiveness and stability. To validate its practical utility, we evaluate FedMate on semantic segmentation tasks using real-world autonomous driving datasets, which confirms its scalability and robustness in complex applications.

2 Related Work

In this section, we critically analyze existing approaches from two fundamental perspectives: the partitioning strategies for personalized modules within local models, and the mechanisms for establishing and integrating generalization-oriented consensus. By discussing the

inherent limitations of these methods, we elucidate the key motivations underlying our proposed approach.

2.1 Personalized Module Partitioning

Traditional FL methods such as FedAvg [25] treat the entire model as a shared component and adopt identical training procedures across clients. MOON [18] conducts contrastive learning within the feature space to drive local models away from their historical states and closer to the current global model. FedProx [19] and Ditto [20], on the other hand, introduce direct parameter-level constraints to regularize local training. Collectively, these methods attempt to utilize a unified global consensus to offer a general update direction for local models facing divergent objectives due to data heterogeneity [39, 33]. Nonetheless, these methods often enforce strong generalization by overwriting local models with the global model prior to training. Under substantial cross-client heterogeneity, selectively incorporating global consensus can better align with diverse client objectives.

Consequently, researchers have explored model partitioning strategies, selectively applying global updates to specific subsets of parameters [29, 11]. This fine-grained approach seeks to enable the output model to more effectively balance global generalization with client-specific personalization. FedCAC [36] conducts layer- and parameter-wise analysis by evaluating the degree of variation in model outputs or loss functions, generating masks to differentiate personalized layers from shared layers. In parallel, FedDecomp [37] decomposes model parameters into the sum of personalized and shared components to achieve a clear separation of personalization and generalization knowledge. Notably, these methods typically introduce additional computational overhead during region partitioning or parameter decomposition. Motivated by the positive effects demonstrated in multi-task learning [2], the strategy of decoupling the model into a feature extractor and a classifier has also garnered increasing attention in the PFL field. FedPer [1] shares only the local feature extractor across clients, while FedRep [7] builds upon FedPer by decoupling the training of the feature extractor and classifier. FedBABU [28] and Fed-RoD [4] further optimize the personalized classifier heads through local fine-tuning and vanilla softmax. However, these approaches offer limited consideration of the coupling between decoupled components and the internal balance of capacities within the classifier.

2.2 Generalization Consensus

To achieve the personalization-aware generalization consensus, methods like FedPAC [38], FedAMP [14], and FedReMa [21] leverage auxiliary local data statistics or model similarity measures to identify analogous clients for personalized aggregation. In addition, category center loss, widely adopted in FL for its representation learning efficacy [34, 13, 24], guides local training with generalization-oriented signals. Recent advances further employ global prototypes as a generalization consensus to regularize local feature learning: FedPAC [38], FedFA [43], and FedProto [31] use prototypes to regularize feature extractor training; FedProc [27] applies them to contrastive learning; and FedPCL [32] integrates them into personalized model learning. Complementary approaches like FedMD [17] and FedKD [35] distill global generalization knowledge into local models via classification-focused optimization. Despite their promising capabilities, these methods often lack robust mechanisms to rigorously assess the quality of uploaded information, which undermines the reliability of the global consensus.

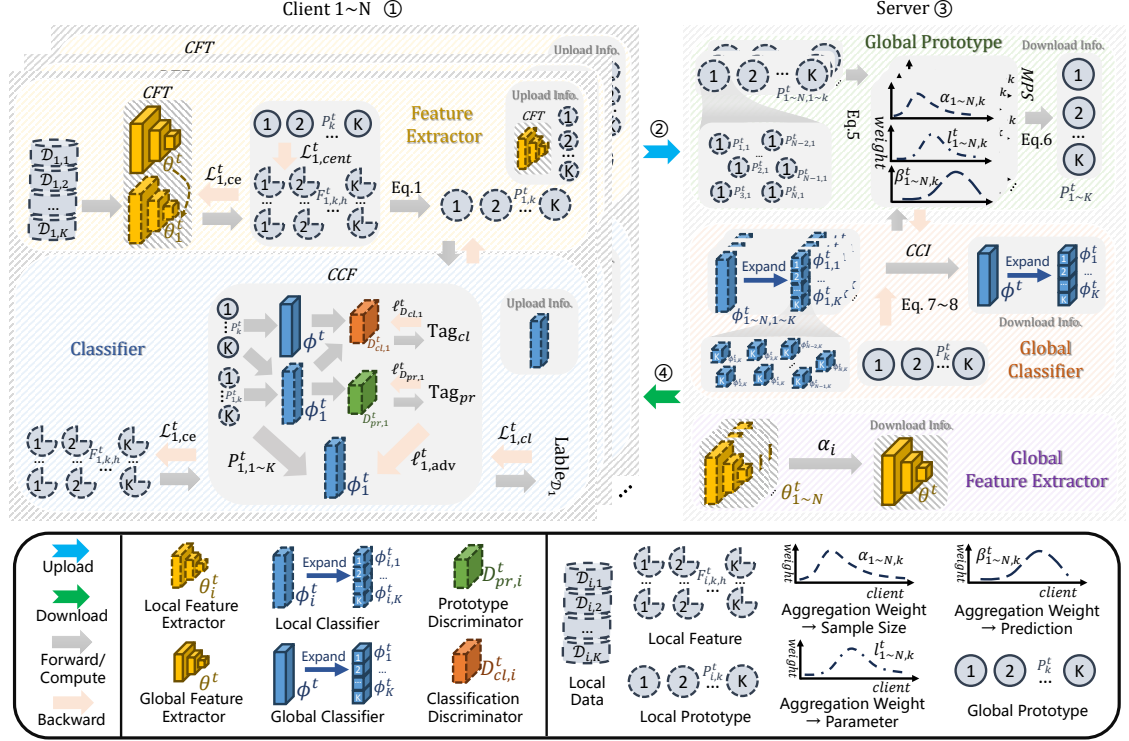


Figure 2. FedMate workflow. ① Local training: Clients train with decoupled objectives (cross-entropy loss, center loss, and dual adversarial learning). ② Selective uploading: Clients upload local classifiers, prototypes, and sample statistics (both total and per-class counts); feature extractors are uploaded only during scheduled rounds. ③ Server aggregation: The server weights multi-view prototypes using relative entropy-based scoring and aggregates classifiers per-class via sample-size-weighted averaging with fine-tuning. ④ Global broadcast: The server distributes updated global classifiers and prototypes to all clients; the global feature extractor is downloaded selectively.

3 Methodology

3.1 Preliminaries and Problem Formulation

Terminology. We consider an FL scenario with N clients, where the union of all local datasets is denoted as \mathcal{D} . The dataset owned by client i is denoted by \mathcal{D}_i , satisfying $\mathcal{D} = \bigcup_{i=1}^N \mathcal{D}_i$. The total dataset \mathcal{D} spans a set of classes \mathcal{C} , where $|\mathcal{C}|$ denotes the total number of classes, and class indices are stored in $[\mathcal{C}]$. Each client i holds a subset of classes denoted as $[\mathcal{C}_i] \subseteq [\mathcal{C}]$. Each sample $(x_i, y_i) \in \mathcal{D}_i$ consists of an input $x_i \in \mathcal{X}$ and a label $y_i \in [\mathcal{C}_i]$, where the input space satisfies $\mathcal{X} \subseteq \mathbb{R}^d$ with d denoting the input dimension. The model of client i is parameterized by w_i , consisting of a feature extractor θ_i and a classifier ϕ_i . The feature extractor $f_i : \mathbb{R}^d \rightarrow \mathbb{R}^K$ maps inputs from \mathcal{X} to a representation space $\mathcal{H} \subseteq \mathbb{R}^K$. For each class $k \in [\mathcal{C}_i]$, the class prototype $P_{i,k}$ is computed as:

$$P_{i,k} = \frac{\sum_{x_{i,k} \in \mathcal{D}_{i,k}} f_i(\theta_i; x_{i,k})}{|\mathcal{D}_{i,k}|}, \quad (1)$$

where $\mathcal{D}_{i,k}$ is the set of local samples from class k . The classifier $g_i : \mathbb{R}^K \rightarrow \mathbb{R}^{|\mathcal{C}|}$ maps feature embeddings to logits over the full label space \mathcal{C} , with final predictions obtained by normalizing the logits. Throughout this paper, the final layer is defined as the classifier, and all preceding layers collectively form the feature extractor.

Loss function and data heterogeneity. This paper studies PFL, where each client retains a model tailored to its local task. The system objective minimizes the weighted average of client-specific losses:

$$\mathcal{L}(W) = \sum_{i=1}^N \alpha_i \frac{\sum_{(x_i, y_i) \in \mathcal{D}_i} \ell_{ce}(\omega_i; x_i, y_i)}{|\mathcal{D}_i|}, \quad \alpha_i = \frac{|\mathcal{D}_i|}{\sum_{j=1}^N |\mathcal{D}_j|}, \quad (2)$$

where $W = \{\omega_1, \omega_2, \dots, \omega_N\}$ is the set of all client models, $\ell_{ce}(\cdot)$ denotes the cross-entropy loss, and α_i is the normalized weight proportional to the normalized $|\mathcal{D}_i|$. For the i -th client, the joint data distribution $\mathbb{P}(x_i, y_i)$ decomposes into: $\mathbb{P}(x_i, y_i) = \mathbb{P}(x_i|y_i)\mathbb{P}(y_i) = \mathbb{P}(y_i|x_i)\mathbb{P}(x_i)$, where $\mathbb{P}(x_i)$ and $\mathbb{P}(y_i)$ are the marginal distributions over the input and label spaces, respectively. We specifically address client-wise label distribution skew, where different clients have distinct marginal label distributions, formally expressed as $\mathbb{P}(y_i) \neq \mathbb{P}(y_j)$ for $i \neq j$. This heterogeneity challenges the learning of robust and generalizable models.

3.2 FedMate Overview

Step 1: Client training. (i) Each client performs supervised training with cross-entropy loss on its local dataset, following a decoupled strategy similar to FedRep [7], where the classifier is trained before the feature extractor. (ii) The feature extractor training incorporates a center loss computed using global prototypes to enhance feature compactness. (iii) The classifier training employs an adversarial loss with dual discriminators to align global and local prototype distributions, treating the classifier as a generator, and a prototype-based cross-entropy loss to maintain knowledge of previous classes and mitigate catastrophic forgetting.

Step 2: Client-to-server upload. Clients upload their local classifier, prototypes, and both total and per-class sample sizes. The local feature extractor is selectively uploaded only when the current round belongs to the predefined subset of rounds Q .

Step 3: Server aggregation. (i) For prototypes, the weights used in aggregation are computed from sample sizes, prototype parameters, and predictions of the previous global classifier, then combined

via relative entropy. (ii) For classifiers, a fine-grained per-class aggregation is performed, weighted by per-class sample sizes. The aggregated classifier is fine-tuned using the latest global prototypes. (iii) If feature extractor parameters are received, they are aggregated weighted by the total sample sizes.

Step 4: Server-to-client download. The server broadcasts the global classifier and prototypes to all clients, while the global feature extractor is only transmitted to clients when the current communication round involves feature extractor aggregation, maintaining synchronization with the conditional upload protocol from Step 2.

This process repeats until convergence or the maximum communication round is reached (see Fig. 2 and Appx. 1 for details).

3.3 Complementary Classification Fusion (CCF)

To effectively fuse complementary classification knowledge, we first differentiate the strengths of global and local classifiers. The global classifier provides balanced knowledge coverage and improved per-class generalization by aggregating cross-client information. In contrast, the local classifier specializes in task-specific adaptation through sustained training on local datasets. Our goal is to leverage the combined knowledge of these classifiers to (i) fill class-specific gaps in the local classifier, (ii) enhance its generalization over existing classes, and (iii) mitigate catastrophic forgetting of local adaptability. Since the global prototype is aggregated from client-specific local prototypes, it inherently reflects the distribution of global tasks, whereas each local prototype captures the task-specific characteristics of its respective client. To retain valuable information from both perspectives, we introduce an adversarial training mechanism that selectively preserves the most beneficial classification knowledge.

Specifically, our approach implements two distinct adversarial training objectives. First, at round t , the global prototypes $P^t = \{P_1^t, P_2^t, \dots, P_{|\mathcal{C}|}^t\}$ and the local prototypes $P_i^t = \{P_{i,k}^t \mid k \in [\mathcal{C}_i]\}$ are input into the local classifier ϕ_i^t . The resulting outputs are then passed to the prototype discriminator $D_{pr,i}$ (a binary discriminator producing probability-valued outputs) trained with loss:

$$\ell_{D_{pr,i}}^t = \sum_{k \in [\mathcal{C}_i]} \left[\log D_{pr,i}(g_i(\phi_i^t; P_k^t)) + \log (1 - D_{pr,i}(g_i(\phi_i^t; P_{i,k}^t))) \right].$$

In the second phase, the global prototypes P^t are evaluated using both the local (ϕ_i^t) and global (ϕ^t) classifiers. The outputs are then assessed by a classification discriminator $D_{cl,i}$ (similarly a binary discriminator yielding probabilistic scores), which minimizes:

$$\ell_{D_{cl,i}}^t = \sum_{k \in [\mathcal{C}_i]} \left[\log D_{cl,i}(g(\phi^t; P_k^t)) + \log (1 - D_{cl,i}(g_i(\phi_i^t; P_k^t))) \right].$$

Accordingly, the local classifier ϕ_i^t serves as the generator in both adversarial processes, guided by feedback from the discriminators:

$$\ell_{i,adv}^t = \sum_{k \in [\mathcal{C}_i]} \log D_{pr,i}(g_i(\phi_i^t; P_{i,k}^t)) + \sum_{k \in [\mathcal{C}_i]} \log D_{cl,i}(g_i(\phi_i^t; P_k^t)),$$

where $\ell_{i,adv}^t$ is the adversarial loss. To further alleviate forgetting, the local prototype P_i^t is introduced as an additional supervisory signal:

$$\ell_{i,ccf}^t = \sum_{k \in [\mathcal{C}_i]} \ell_{ce}(\phi_i^t; P_{i,k}^t, y_{i,k}) + \kappa_{cl}^t \ell_{i,adv}^t, \quad \kappa_{cl}^t = 1 - \frac{t}{t_{\max}},$$

where $\ell_{i,ccf}^t$ is the CCF component loss, and κ_{cl}^t is a weighting factor that balances the adversarial loss. For stabilize early training, κ_{cl}^t is adjusted based on the current round t and the maximum round t_{\max} . The overall loss for training the local classifier is then given by:

$$\ell_{i,cl}^t = \sum_{(x_i, y_i) \in \mathcal{D}_i} \ell_{ce}(\omega_i^t; x_i, y_i) + \lambda_c \ell_{i,ccf}^t, \quad (3)$$

where the hyperparameter λ_c controls the contribution of $\ell_{i,ccf}^t$. A detailed description of the CCF input–output workflow is in Appx. 3.

3.4 Cost-aware Feature Transmission (CFT)

When the global prototypes possess constrained representational capacity (e.g., due to low-dimensional embeddings), their effectiveness in guiding local feature extractor training becomes limited. Prior solutions like FedPAC [38] and FedFA [43] attempt to mitigate this by transmitting both global feature extractors and prototypes to clients, forcibly overwriting local extractors before prototype-based supervision. While this strategy improves global model consistency, it introduces substantially increased communication overhead from frequent extractor transfers and potential degradation of local model personalization due to overwriting of client-specific features.

Motivated by these limitations, we propose a cost-aware selective communication strategy for feature extractor transmission. Our approach dynamically schedules transmissions based on the information ratio between prototypes and the feature extractor, thereby reducing unnecessary communication overhead while balancing the generalization–personalization trade-off for local models. To enhance deployability, we quantify information content using parameter counts, defining the information ratio q between prototypes and feature extractor as:

$$q = \frac{Par(\theta_i^t)}{Par\left(\sum_{k \in [\mathcal{C}_i]} P_k^t\right)}, \quad (4)$$

where $Par(\cdot)$ denotes the parameter count function. The feature extractor is selectively uploaded at rounds that are not multiples of $x \times q$, maintaining equivalent total communication costs to per-round model uploading. In this paper, we collect the selected rounds into a scheduling set Q .

3.5 Multi-view Prototype Scrutiny (MPS)

As discussed in Section 1, determining prototype aggregation weights based solely on local sample sizes may yield suboptimal global representations. To address this, we propose a multi-faceted weight calibration approach that jointly considers: sample sizes, prototype parameters, and predictions from the previous global classifier. This integrated weighting scheme promotes a more robust and unbiased global consensus during prototype aggregation.

For each class $k \in [\mathcal{C}_i]$, we compute three complementary weighting components: (i) sample-size-based $\alpha_{i,k}$, determined by the sample size $|\mathcal{D}_{i,k}|$; (ii) centroid-similarity-based $l_{i,k}^t$, obtained by the cosine similarity sim between each local prototype and its parameter centroid An_k^t ; and (iii) prediction-based $\beta_{i,k}^t$, derived from logit-based evaluation of each prototype using the previous global classifier ϕ^{t-1} . These weights are defined as:

$$\alpha_{i,k} = \frac{|\mathcal{D}_{i,k}|}{\sum_{j \in \mathcal{B}_k} |\mathcal{D}_{j,k}|},$$

$$l_{i,k}^t = \frac{\text{sim}(P_{i,k}^t, An_k^t)}{\sum_{j \in \mathcal{B}_k} \text{sim}(P_{j,k}^t, An_k^t)},$$

$$\beta_{i,k}^t = \frac{g(\phi_k^{t-1}, P_{i,k}^t)}{\sum_{j \in \mathcal{B}_k} g(\phi_k^{t-1}, P_{j,k}^t)}, \quad (5)$$

where $An_k^t = \frac{\sum_{i \in \mathcal{B}_k} P_{i,k}^t}{|\mathcal{B}_k|}$ with \mathcal{B}_k denoting the set of clients with local prototypes for class k , and ϕ_k^{t-1} is the k -th class neuron parameters of global classifier.

Then, we compute pairwise Jensen-Shannon (JS) divergences between the three weight sets $\mathcal{S}_{i,k}^t = \{\alpha_{i,k}, l_{i,k}^t, \beta_{i,k}^t\}$, requiring only three comparisons due to JS symmetry. These divergences are aggregated into a consensus weighting term W_{mps} :

$$W_{i,k,\text{mps}}^t = \text{Softmax} \left(- \left\{ \sum_{s' \neq s} \text{JS}(s, s') \mid s \in \mathcal{S}_{i,k}^t \right\} \right).$$

Smaller JS divergence yields larger normalized weights, penalizing deviant components. The final aggregation weight combines all three components:

$$W_{i,k,\text{final}}^t = W_{i,k,\text{mps}_1}^t \cdot \alpha_{i,k} + W_{i,k,\text{mps}_2}^t \cdot l_{i,k}^t + W_{i,k,\text{mps}_3}^t \cdot \beta_{i,k}^t,$$

where W_{i,k,mps_h}^t denotes the h -th element of $W_{i,k,\text{mps}}^t$. Now we obtain the aggregated global prototype as:

$$P_k^t = \sum_{i \in \mathcal{B}_k} W_{i,k,\text{final}}^t \cdot P_{i,k}^t. \quad (6)$$

3.6 Category-wise Classifier Integration (CCI)

In classification architectures, output neurons in the classifier is inherently linked to a specific class, serving as a direct predictor for that category. Conventional aggregation methods typically process the classifier holistically, disregarding this intrinsic neuron-class alignment. Such coarse-grained fusion risks introducing bias toward client-specific dominant categories, particularly under heterogeneous data conditions where class samples are unevenly distributed across clients. To address this, we propose the CCI scheme, which performs neuron-level aggregation aligned with class boundaries. This fine-grained approach enables more targeted and unbiased parameter fusion, reducing the impact of client-side data heterogeneity and refining each category's decision boundary based on available knowledge.

For each class k , we aggregate the corresponding classifier neuron parameters across clients by sample-size-proportional weighting:

$$\phi_k^t = \alpha_{i,k} \cdot \phi_{i,k}^t. \quad (7)$$

Furthermore, to harmonize the decoupled training of feature extractors and classifiers, we enforce consistency between the global prototypes (class-level feature centroids) and the global classifier. While prototypes guide feature extractor learning and classifier parameters direct local optimization, their alignment ensures coherent joint evolution of the feature-classification pipeline. This prevents objective drift between modules during the FL process. Specifically, the global classifier is fine-tuned using the current global prototypes:

$$\phi_k^t \leftarrow \phi_k^t - \eta \nabla_{\phi} \ell_{\text{ce}}(\phi_k^t; P_k^t, y_k), \quad (8)$$

where η is the fine-tuning learning rate. This prototype-aware refinement aligns decision boundaries with evolving feature clusters, maintaining coupling between the feature extractor and classifier despite local decoupled training.

4 Experiments

In this section, we present key experimental results evaluating the generalization, adaptability, stability, and scalability of our method. Additional analyses of convergence, communication costs, and hyperparameter sensitivity are provided in Appx. 2.

4.1 Experimental Setup

Datasets. We evaluate our method's generalization and robustness across six benchmark datasets spanning varying complexity levels: CIFAR-10 [16], CINIC-10 [10], Animal-10 [9], EMNIST [6], CIFAR-100 [16], and Cityscapes [8]. These datasets differ in input dimensionality, label granularity, and visual complexity, offering a comprehensive foundation for performance evaluation.

Implementation details. We employ dataset-specific architectures with modular feature extractors and classifiers: CIFAR-10 and CINIC-10 use a 3-Conv-2-FC CNN (following FedPAC [38]); Animal-10 adopts an enhanced 3-Conv-2-FC variant with larger filters for natural images; EMNIST utilizes a compact 2-Conv design; CIFAR-100 implements a deeper 4-Conv network; and Cityscapes employs BiSeNetV2 for segmentation, demonstrating scalability to deeper, dense prediction tasks. Additionally, following established protocols from SCAFFOLD [15] and FedAMP [14], we construct client datasets with controlled class imbalance through a tunable parameter $s \in [0, 100]$: $s\%$ of each client's training data follows uniform class distribution, while the remaining $(100 - s)\%$ exhibits bias toward randomly selected dominant classes. Crucially, all clients share an identically structured test set with balanced class distribution and equivalent total samples (matching training set size), ensuring evaluation reflects true generalization across the complete label space rather than local data biases. This design mimics realistic scenarios where future data distributions are unknown.

Comparison baselines. We evaluate against three categories of FL approaches: 1) traditional FL methods, including FT-FedAvg [25] (post-training fine-tuning) and MOON [18] (contrastive representation alignment); 2) prototype-based methods, such as FedFA [43] (joint extractor-classifier regularization) and Fed-Proto [31] (prototype-only aggregation); and 3) model-decoupling approaches, comprising LG-FedAvg [22] (personalized extractors), FedPer [1]/FedRep [7] (personalized classifiers with shared extractors, where FedRep additionally decouples training phases), Fed-BABU [28] (phased classifier freezing), and FedPAC [38] (statistics-augmented personalization). For segmentation tasks, we include Fed-Seg [26] (contrastive-enhanced representation learning). All classification experiments report mean accuracy (%).

4.2 Main Results

Generalization performance evaluation. Our comprehensive experiments assess model generalization under varying data heterogeneity levels (Tab. 1). Key findings reveal: 1) our method consistently outperforms the baselines across datasets and heterogeneity scenarios; 2) standard model-decoupling PFL approaches (e.g., LG-FedAvg, FedPer, and FedRep) show limited effectiveness in global complementary knowledge integration; 3) prototype-only methods (FedProto) demonstrate the inherent limitations of low-dimensional guidance (suffering a >15% performance degradation compared to our approach); 4) our CCF mechanism enforces moderate global constraints during local training, enabling more effective knowledge integration and reducing overfitting.

Method	CIFAR-10				CINIC-10		EMNIST	
	s = 10	s = 30	s = 50	s = 70	s = 10	s = 70	s = 10	s = 70
Local	28.61 \pm 0.06	36.08 \pm 0.07	40.51 \pm 0.05	42.40 \pm 0.04	22.86 \pm 0.03	29.95 \pm 0.04	31.02 \pm 0.09	50.84 \pm 0.08
FT-FedAvg	49.39 \pm 0.07	57.55 \pm 0.09	61.95 \pm 0.08	64.33 \pm 0.06	32.72 \pm 0.06	40.55 \pm 0.07	59.03 \pm 0.11	69.24 \pm 0.05
FedProto	29.91 \pm 0.04	38.45 \pm 0.07	43.54 \pm 0.08	46.27 \pm 0.10	22.19 \pm 0.02	30.15 \pm 0.04	31.72 \pm 0.09	57.14 \pm 0.06
LG-FedAvg	28.32 \pm 0.05	35.79 \pm 0.06	40.91 \pm 0.04	42.37 \pm 0.11	22.57 \pm 0.04	29.14 \pm 0.03	31.71 \pm 0.05	53.64 \pm 0.04
FedPer	33.93 \pm 0.06	42.39 \pm 0.05	47.49 \pm 0.07	51.43 \pm 0.10	24.64 \pm 0.05	32.60 \pm 0.03	36.39 \pm 0.06	54.97 \pm 0.07
FedRep	38.97 \pm 0.09	47.63 \pm 0.10	52.53 \pm 0.05	53.51 \pm 0.06	26.64 \pm 0.03	33.92 \pm 0.04	34.08 \pm 0.09	55.47 \pm 0.08
FedBABU	45.05 \pm 0.08	56.25 \pm 0.07	60.89 \pm 0.06	64.87 \pm 0.05	27.45 \pm 0.12	37.12 \pm 0.03	30.69 \pm 0.08	46.23 \pm 0.06
FedPAC	53.02 \pm 0.06	65.42 \pm 0.08	69.97 \pm 0.07	71.08 \pm 0.04	35.67\pm0.05	49.09 \pm 0.07	56.71 \pm 0.09	70.14 \pm 0.06
Ours	55.05\pm0.02	68.13\pm0.11	70.21\pm0.02	72.19\pm0.06	34.98 \pm 0.02	50.24\pm0.06	60.29\pm0.03	72.15 \pm0.10
Backbone	39.11 \pm 0.05	48.17 \pm 0.10	52.51 \pm 0.06	54.20 \pm 0.08	26.33 \pm 0.11	33.95 \pm 0.02	35.47 \pm 0.05	55.37 \pm 0.08
+MPS+CFT	50.17 \pm 0.10	59.22 \pm 0.05	63.26 \pm 0.08	66.75 \pm 0.06	29.66 \pm 0.03	45.07 \pm 0.05	52.49 \pm 0.05	67.33 \pm 0.07
+CCI+CCF	52.17 \pm 0.03	62.15 \pm 0.09	62.89 \pm 0.12	64.97 \pm 0.03	30.02 \pm 0.08	44.27 \pm 0.08	54.17 \pm 0.11	66.57 \pm 0.05

Table 1. Generalization performance evaluation under varying heterogeneity settings (controlled by s).

Method	CIFAR-10	CINIC-10	CIFAR-100
Local	65.15 \pm 0.08	55.21 \pm 0.12	35.27 \pm 0.14
FT-FedAvg	90.65 \pm 0.07	84.12 \pm 0.03	70.51 \pm 0.10
MOON	66.67 \pm 0.12	57.37 \pm 0.06	37.29 \pm 0.09
FedProto	85.21 \pm 0.04	81.61 \pm 0.11	75.28 \pm 0.06
FedFA	84.19 \pm 0.13	80.86 \pm 0.09	71.59 \pm 0.07
LG-FedAvg	88.35 \pm 0.05	82.10 \pm 0.06	70.95 \pm 0.12
FedPer	91.21 \pm 0.09	85.05 \pm 0.07	69.97 \pm 0.10
FedRep	91.45 \pm 0.02	85.88 \pm 0.08	75.33 \pm 0.11
FedBABU	88.83 \pm 0.10	81.65 \pm 0.13	67.71 \pm 0.12
FedPAC	91.71 \pm 0.06	84.28 \pm 0.09	74.24 \pm 0.08
Ours	92.18\pm0.13	86.01\pm0.10	77.04\pm0.05

Table 2. Adaptability evaluation under extreme heterogeneity settings.

Ablation analysis. We systematically evaluate component contributions under identical heterogeneous conditions. The results are shown in the lower half of Tab. 1, which demonstrates that both feature extractor modules (MPS and CFT) and classifier components (CCI and CCF) contribute significantly to model performance, with their combined removal degrading accuracy by 3%-17% across datasets. Notably, under extreme heterogeneity ($s \leq 10$), introducing moderate global constraints at the classifier level substantially improves generalization, aligning with our objective stated in Section 1: achieving a balance between global generalization and local personalization through structurally decoupled yet functionally coordinated modules.

Local adaptability evaluation. To evaluate the models’ adaptability to local tasks, we consider an extreme pathological heterogeneity scenario where each client holds data from a subset of classes (3 classes for CIFAR-10 and CINIC-10, 10 classes for CIFAR-100), with test sets matching local data distributions. Our method demonstrates superior adaptability across datasets of varying difficulty (Tab. 2) through two key design aspects: 1) selective inte-

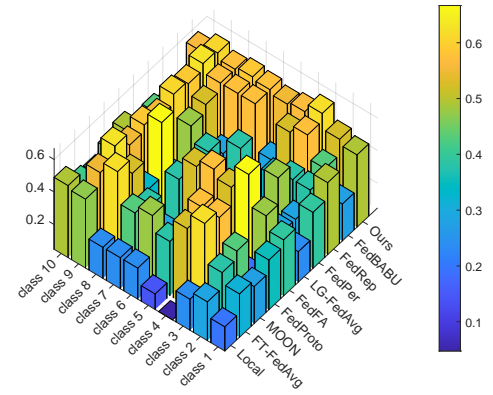


Figure 3. Class-wise accuracy on Animal-10.

gration of global feature extractors (avoiding full overwrites) preserves local feature specialization while enabling controlled knowledge transfer; and 2) prototype-augmented classifier guidance (combining global classifiers with local prototypes) prevents catastrophic forgetting of personalized knowledge. This dual mechanism achieves a performance gain close to 2% over baselines on the challenging CIFAR-100 dataset while maintaining the critical generalization-personalization balance.

Class-wise accuracy analysis. We evaluate per-class performance on the Animal-10 dataset (high inter-class similarity) using personalized models trained under data heterogeneity $s = 20$, with uniformly distributed test sets. As shown in Fig. 3, standard methods like FedRep and FedPer exhibit strong performance on locally abundant classes but fail on underrepresented ones, reflecting their inability to correct for biased client uploads during global aggregation. Our approach dynamically adjusts aggregation weights using MPS and incorporates class-wise fine-grained aggregation for the classifier, achieving balanced accuracy across all classes.

Stability and robustness analysis. To evaluate the stability of feature extractors and their ability to capture intrinsic class knowledge, we train models on the CINIC-10 dataset under data heterogeneity $s = 20$ and visualize the local prototypes. As shown in Fig. 4, existing methods (FedFA, FedProto, FedPAC) exhibit prototype overlap

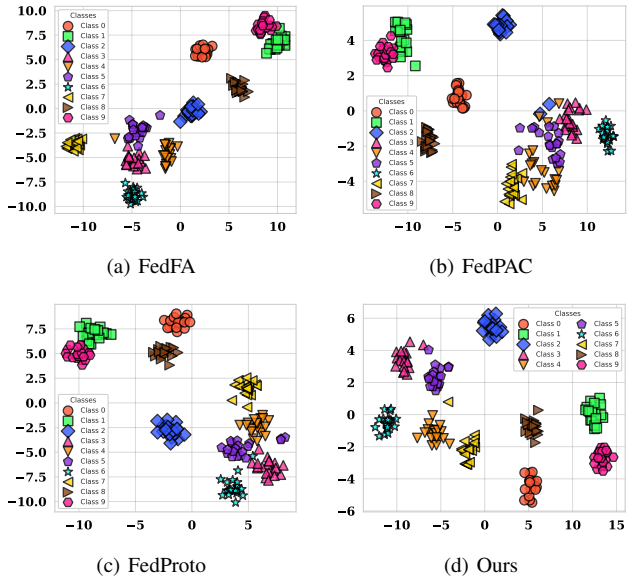


Figure 4. Visualization of the local prototypes using t-SNE.

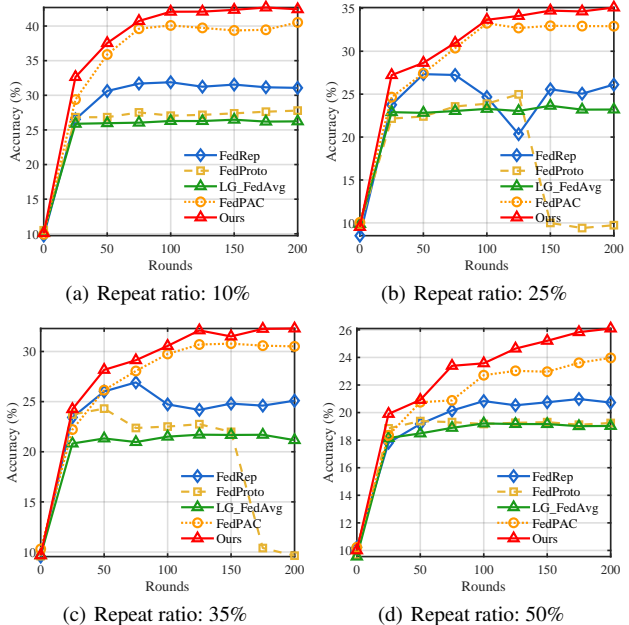


Figure 5. Test accuracy with varying repeat ratios on CINIC-10 ($s = 50$).

among highly confusable classes (e.g., cat, deer, and dog), indicating suboptimal class separation in the embedding space. In contrast, our method employs a more robust global prototype construction mechanism, which enhances consistency during local training and improves the learning of intrinsic class characteristics.

To further examine the effectiveness of the MPS component, we introduce controlled redundancy by selecting a subset of clients based on a predefined repeat ratio. The datasets of these clients contain identical samples replicated multiple times. Experimental results (Fig. 5) demonstrate that our method maintains stable performance across varying redundancy levels. Comparatively, FedProto and FedRep exhibit overfitting tendencies. This underscores the importance of fairly evaluating uploaded client information and forming an unbiased consensus.

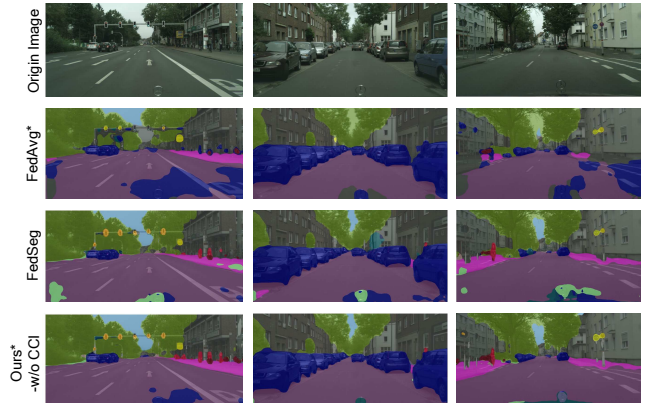


Figure 6. Semantic segmentation performance analysis. Asterisk (*) denotes methods using FedSeg-optimized cross-entropy loss; "-w/o" indicates component removed.

Method	Client 95		Client 152		Client 285	
	mIoU	Acc	mIoU	Acc	mIoU	Acc
FedAvg*	27.23	62.77	35.28	64.17	36.87	65.39
FedSeg	31.27	66.95	37.33	68.01	39.19	68.98
Ours*	32.17	68.79	39.17	69.91	40.28	70.69

Table 3. Segmentation performance comparison (%) on Cityscapes.

Real-world scalability analysis. Following FedSeg, we partition the Cityscapes dataset into 152 clients, distributing 19 semantic classes such that each class is assigned to 8 clients. This setup ensures a highly heterogeneous data distribution, as each client contains data from only a single class.

As shown in Fig. 6, FedAvg struggles with certain categories (e.g., "person"), likely due to inadequate representation-level alignment. While FedSeg improves consistency through feature contrastive learning, it still underperforms on fine-grained or structurally complex targets. In contrast, our approach introduces a quality-aware aggregation strategy that adaptively adjusts client contributions, fostering more structured global prototypes. This enhancement yields comparatively clearer segmentation boundaries, particularly for challenging classes like "person", "building", and "traffic sign". We further evaluate our method through segmentation experiments under varying client-per-class configurations. As shown in Tab. 3, our approach consistently outperforms baselines, achieving higher mean IoU (prediction-ground truth overlap) and mean accuracy scores.

5 Conclusion

In this paper, we propose FedMate, a novel FL framework that facilitates complementary knowledge fusion through recalibrated prototype guidance and merit-based discrimination training. Our approach achieves bilateral optimization across server and client objectives: On the server side, the MPS strategy strengthens global guidance via aggregation recalibration, while CCI refines supervisory signals to ensure consistency; on the client side, a dual-adversarial mechanism enhances both inter-class separability and cross-client generalization. Empirical results demonstrate that FedMate effectively synergizes its decoupled components, striking a superior balance between global generalization and local personalization compared to existing methods. For future work, we plan to scale FedMate to larger-scale, real-world heterogeneous scenarios, explore adaptive coordination mechanisms for decoupled components, and reduce peak communication costs per round to improve practical usability.

Acknowledgments

This work was supported in part by the Taishan Scholars Program under Grants tsqn202211203 and tsqn202408239, in part by the NSFC under Grant 62402256, in part by the Shandong Provincial Nature Science Foundation of China under Grant ZR2024MF100, and in part by the QLU/SDAS Pilot Project for Integrated Innovation of Science, Education, and Industry under Grant 2024ZDZX08.

References

[1] M. G. Arivazhagan, V. Aggarwal, A. K. Singh, and S. Choudhary. Federated learning with personalization layers. *arXiv preprint arXiv:1912.00818*, 2019.

[2] Y. Bengio, A. Courville, and P. Vincent. Representation learning: A review and new perspectives. *IEEE Transactions on Pattern Analysis and Machine Intelligence*, 35(8):1798–1828, 2013.

[3] Z. Charles, G. Teston, L. Dery, K. Rush, N. Fallen, Z. Garrett, A. Szlam, and A. Douillard. Communication-efficient language model training scales reliably and robustly: Scaling laws for diloco. *arXiv preprint arXiv:2503.09799*, 2025.

[4] H. Chen and W. Chao. On bridging generic and personalized federated learning for image classification. In *International Conference on Learning Representations*, 2022.

[5] S. Cheng, J. Wu, Y. Xiao, and Y. Liu. FedGEMS: Federated learning of larger server models via selective knowledge fusion. *arXiv preprint arXiv:2110.11027*, 2021.

[6] G. Cohen, S. Afshar, J. Tapson, and A. Van Schaik. EMNIST: Extending mnist to handwritten letters. In *International Joint Conference on Neural Networks*, pages 2921–2926. IEEE, 2017.

[7] L. Collins, H. Hassani, A. Mokhtari, and S. Shakkottai. Exploiting shared representations for personalized federated learning. In *International Conference on Machine Learning*, pages 2089–2099. PMLR, 2021.

[8] M. Cordts, M. Omran, S. Ramos, T. Rehfeld, M. Enzweiler, R. Benenson, U. Franke, S. Roth, and B. Schiele. The cityscapes dataset for semantic urban scene understanding. In *Proceedings of the IEEE/CVF Conference on Computer Vision and Pattern Recognition*, pages 3213–3223, 2016.

[9] A. Corrado. Animals-10 dataset, 2018. URL <https://www.kaggle.com/datasets/alessiocorrado99/animals10>.

[10] L. N. Darlow, E. J. Crowley, A. Antoniou, and A. J. Storkey. Cinic-10 is not imagenet or cifar-10. *arXiv preprint arXiv:1810.03505*, 2018.

[11] D. Deng, X. Wu, T. Zhang, X. Tang, H. Du, J. Kang, J. Liu, and D. Niyato. Fedasa: A personalized federated learning with adaptive model aggregation for heterogeneous mobile edge computing. *IEEE Transactions on Mobile Computing*, 2024.

[12] Y. Deng, M. M. Kamani, and M. Mahdavi. Adaptive personalized federated learning. *arXiv preprint arXiv:2003.13461*, 2020.

[13] C. Florea, M. Badea, L. Florea, A. Racoviteanu, and C. Vertan. Marginmix: Semi-supervised learning for face expression recognition. In *European Conference on Computer Vision*, pages 1–17, 2020.

[14] Y. Huang, L. Chu, Z. Zhou, L. Wang, J. Liu, J. Pei, and Y. Zhang. Personalized cross-silo federated learning on non-iid data. In *Proceedings of the AAAI Conference on Artificial Intelligence*, volume 35, pages 7865–7873, 2021.

[15] S. P. Karimireddy, S. Kale, M. Mohri, S. Reddi, S. Stich, and A. T. Suresh. Scaffold: Stochastic controlled averaging for federated learning. In *International Conference on Machine Learning*, pages 5132–5143. PMLR, 2020.

[16] A. Krizhevsky, G. Hinton, et al. Learning multiple layers of features from tiny images. 2009.

[17] D. Li and J. Wang. Fedmd: Heterogenous federated learning via model distillation. *arXiv preprint arXiv:1910.03581*, 2019.

[18] Q. Li, B. He, and D. Song. Model-contrastive federated learning. In *Proceedings of the IEEE/CVF Conference on Computer Vision and Pattern Recognition*, pages 10713–10722, 2021.

[19] T. Li, A. K. Sahu, M. Zaheer, M. Sanjabi, A. Talwalkar, and V. Smith. Federated optimization in heterogeneous networks. *Proceedings of Machine Learning and Systems*, 2:429–450, 2020.

[20] T. Li, S. Hu, A. Beirami, and V. Smith. Ditto: Fair and robust federated learning through personalization. In *International Conference on Machine Learning*, pages 6357–6368. PMLR, 2021.

[21] H. Liang, Z. Zhan, W. Liu, X. Zhang, C. W. Tan, and X. Chen. FedReMa: Improving personalized federated learning via leveraging the most relevant clients. In *European Conference on Artificial Intelligence*, pages 2090–2097, 2024.

[22] P. P. Liang, T. Liu, L. Ziyin, N. B. Allen, R. P. Auerbach, D. Brent, R. Salakhutdinov, and L.-P. Morency. Think locally, act globally: Federated learning with local and global representations. *arXiv preprint arXiv:2001.01523*, 2020.

[23] W. Liang, G. A. Tadesse, D. Ho, L. Fei-Fei, M. Zaharia, C. Zhang, and J. Zou. Advances, challenges and opportunities in creating data for trustworthy ai. *Nature Machine Intelligence*, 4(8):669–677, 2022.

[24] Y. Liu, Y. Tian, Y. Zhao, H. Yu, L. Xie, Y. Wang, Q. Ye, J. Jiao, and Y. Liu. Vmamba: Visual state space model. *Advances in Neural Information Processing Systems*, 37:103031–103063, 2024.

[25] B. McMahan, E. Moore, D. Ramage, S. Hampson, and B. A. y Arcas. Communication-efficient learning of deep networks from decentralized data. In *Artificial Intelligence and Statistics*, pages 1273–1282. PMLR, 2017.

[26] J. Miao, Z. Yang, L. Fan, and Y. Yang. Fedseg: Class-heterogeneous federated learning for semantic segmentation. In *Proceedings of the IEEE/CVF Conference on Computer Vision and Pattern Recognition*, pages 8042–8052, 2023.

[27] X. Mu, Y. Shen, K. Cheng, X. Geng, J. Fu, T. Zhang, and Z. Zhang. Fedproc: Prototypical contrastive federated learning on non-iid data. *Future Generation Computer Systems*, 143:93–104, 2023.

[28] J. Oh, S. Kim, and S.-Y. Yun. FedBABU: Toward enhanced representation for federated image classification. In *International Conference on Learning Representations*, 2022.

[29] K. Pillutla, K. Malik, A.-R. Mohamed, M. Rabbat, M. Sanjabi, and L. Xiao. Federated learning with partial model personalization. In *International Conference on Machine Learning*, pages 17716–17758. PMLR, 2022.

[30] P. Qi, D. Chiaro, and F. Piccialli. Small models, big impact: A review on the power of lightweight federated learning. *Future Generation Computer Systems*, page 107484, 2024.

[31] Y. Tan, G. Long, L. Liu, T. Zhou, Q. Lu, J. Jiang, and C. Zhang. Fedproto: Federated prototype learning across heterogeneous clients. In *Proceedings of the AAAI Conference on Artificial Intelligence*, volume 36, pages 8432–8440, 2022.

[32] Y. Tan, G. Long, J. Ma, L. Liu, T. Zhou, and J. Jiang. Federated learning from pre-trained models: A contrastive learning approach. *Advances in Neural Information Processing Systems*, 35:19332–19344, 2022.

[33] L. Wang, X. Zhang, H. Su, and J. Zhu. A comprehensive survey of continual learning: Theory, method and application. *IEEE Transactions on Pattern Analysis and Machine Intelligence*, 2024.

[34] Y. Wen, K. Zhang, Z. Li, and Y. Qiao. A discriminative feature learning approach for deep face recognition. In *European Conference on Computer Vision*, pages 499–515, 2016.

[35] C. Wu, F. Wu, L. Lyu, Y. Huang, and X. Xie. Communication-efficient federated learning via knowledge distillation. *Nature Communications*, 13(1):2032, 2022.

[36] X. Wu, X. Liu, J. Niu, G. Zhu, and S. Tang. Bold but cautious: Unlocking the potential of personalized federated learning through cautiously aggressive collaboration. In *Proceedings of the IEEE/CVF International Conference on Computer Vision*, pages 19375–19384, 2023.

[37] X. Wu, X. Liu, J. Niu, H. Wang, S. Tang, G. Zhu, and H. Su. Decoupling general and personalized knowledge in federated learning via additive and low-rank decomposition. In *Proceedings of the 32nd ACM International Conference on Multimedia*, pages 7172–7181, 2024.

[38] J. Xu, X. Tong, and S.-L. Huang. Personalized Federated Learning with Feature Alignment and Classifier Collaboration. In *International Conference on Learning Representations*, 2023.

[39] M. Ye, X. Fang, B. Du, P. C. Yuen, and D. Tao. Heterogeneous federated learning: State-of-the-art and research challenges. *ACM Computing Surveys*, 56(3):1–44, 2023.

[40] Q. Yu, Y. Liu, Y. Wang, K. Xu, and J. Liu. Multimodal Federated Learning via Contrastive Representation Ensemble. In *International Conference on Learning Representations*, 2023.

[41] C. Zhang, Y. Xie, H. Bai, B. Yu, W. Li, and Y. Gao. A survey on federated learning. *Knowledge-Based Systems*, 216:106775, 2021.

[42] J. Zhang, Y. Hua, H. Wang, T. Song, Z. Xue, R. Ma, J. Cao, and H. Guan. Gpfl: Simultaneously learning global and personalized feature information for personalized federated learning. In *Proceedings of the IEEE/CVF International Conference on Computer Vision*, pages 5041–5051, 2023.

[43] T. Zhou, J. Zhang, and D. H. Tsang. Fedfa: Federated learning with feature anchors to align features and classifiers for heterogeneous data. *IEEE Transactions on Mobile Computing*, 23(6):6731–6742, 2023.

Appendix

1 Algorithm Details

This section provides the pseudocode for FedMate, supplementing the main text. Algorithm 1 describes the server-side aggregation process, while Algorithm 2 specifies the client-level training procedure.

Algorithm 1 FedMate: Server-side Aggregation Procedure

```

1: Input: Total rounds  $T$ , number of clients  $N$ , learning rate  $\eta$ 
2: Initialize global feature extractor  $\theta^0$  and global classifier  $\phi^0$ 
3: for each round  $t = 0, 1, \dots, T - 1$  do
4:   Server selects a subset  $\mathcal{Z}_t$  of clients
5:   for each client  $i \in \mathcal{Z}_t$  in parallel do
6:     # CT is Client-Training( $\cdot$ )
7:     if  $t = 0$  then
8:        $(\phi_i^{t+1}, P_i^{t+1}, \theta_i^{t+1}(\text{by } Q)) \leftarrow \text{CT}(\theta^t, \phi^t)$ 
9:     else
10:       $(\phi_i^{t+1}, P_i^{t+1}, \theta_i^{t+1}(\text{by } Q)) \leftarrow \text{CT}(\theta^t(\text{if have}), \phi^t, P^t)$ 
11:    end if
12:   end for
13:   Server aggregates  $\{P_i^{t+1}\}$  by Eq. (6) to obtain  $P^{t+1}$ 
14:   Server aggregates  $\{\phi_i^{t+1}\}$  via Eq. (7) and fine-tunes by Eq. (8)
15:   to obtain  $\phi^{t+1}$ 
16:   if feature extractors  $\{\theta_i^{t+1}\}$  are uploaded then
17:     Server aggregates  $\{\theta_i^{t+1}\}$  weighted by  $\alpha_i$  to obtain  $\theta^{t+1}$ 
18:   end if
19: end for

```

Algorithm 2 FedMate: Client-level Training Procedure

```

1: Input: Local epochs  $E$ , feature extractor  $\theta^t$ , classifier  $\phi^t$ , global
   prototype  $P^t$ , hyperparameter  $\lambda_e, \lambda_c$ , learning rate  $\eta_l$ 
2: if received  $\theta^t$  then
3:   Update local feature extractor:  $\theta_i^t \leftarrow \theta^t$ 
4: end if
5: Compute local prototype  $P_i^t$ 
6: for each local epoch  $e = 1, \dots, E$  do
7:   # Freeze feature extractor, train classifier
8:   Train  $\phi_i^t$  by minimizing the loss in Eq. (3)
9:   # Freeze classifier, train feature extractor
10:  if received  $P^t$  then
11:     $\ell_{i, \text{cent}}^t = \sum_{k \in [C_i]} \mathbb{L}_2(\sum_{x_{i,k} \in \mathcal{D}_{i,k}} f_i(\theta_i^t; x_{i,k}); P_k^t)$ 
12:    Train  $\theta_i^t$  by minimizing  $\sum_{(x_i, y_i) \in \mathcal{D}_i} \ell_{\text{ce}}(\omega_i^t; x_i, y_i) + \lambda_e \ell_{i, \text{cent}}^t$ 
13:  end if
14: end for
15: Recompute local prototype  $P_i^{t+1}$ 
16: Return  $(\phi_i^{t+1}, P_i^{t+1}, \theta_i^{t+1}(\text{uploaded only if } t + 1 \in Q))$ 

```

2 Additional Experimental Results

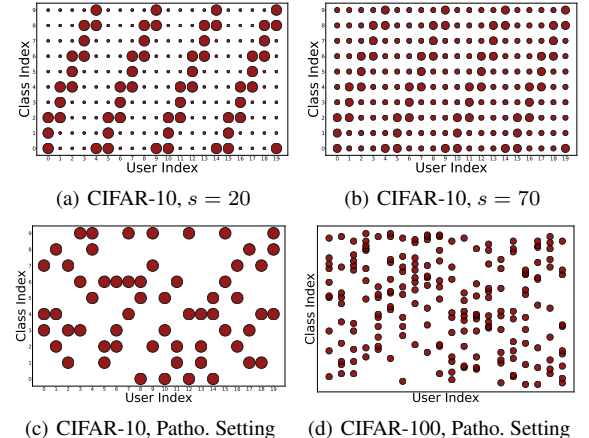


Figure 1. Data distribution under different heterogeneous scenarios.

Data distribution visualization. To better characterize the heterogeneous learning scenarios under investigation, Fig. 1 illustrates the data distributions in extreme pathological (Patho.) settings across different datasets, and under varying degrees of skewness ($s\%$).

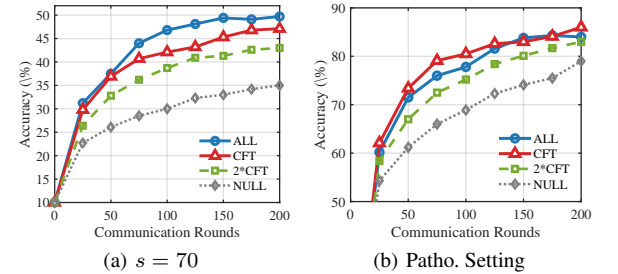


Figure 2. Accuracy curves under different feature extractor transmission strategies: ALL transmits every round, CFT follows the predefined Q , 2*CFT transmits half of Q , and NULL disables transmission.

CFT component evaluation. We evaluate our approach on the CINIC-10 dataset under two conditions: 1) a uniform test distribution (training: $s = 70$) and 2) a heterogeneous test distribution matching the training set (training: Patho.). As shown in Fig. 2(a) and Fig. 2(b), CFT effectively balances model performance with communication efficiency by strategically uploading local feature extractors at appropriate rounds. The results demonstrate that CFT achieves superior performance on the heterogeneous test set (which better reflects real-world local data distributions) compared to transmitting feature extractors in every round (ALL). This improvement stems

from CFT’s ability to relax strict global generalization requirements, thereby achieving a more favorable balance between generalization and personalization. Notably, the selective transmission mechanism based on the predefined threshold Q reduces communication overhead while maintaining model effectiveness.

Convergence analysis. We examine the convergence properties of our method under heterogeneous training conditions ($s = 20$) across datasets with varying complexity levels. Fig. 3 presents the training dynamics, comparing model loss before and after local updates. The results demonstrate that our approach achieves consistent and stable convergence within approximately 150 communication rounds for all evaluated datasets, indicating robust performance regardless of dataset difficulty.

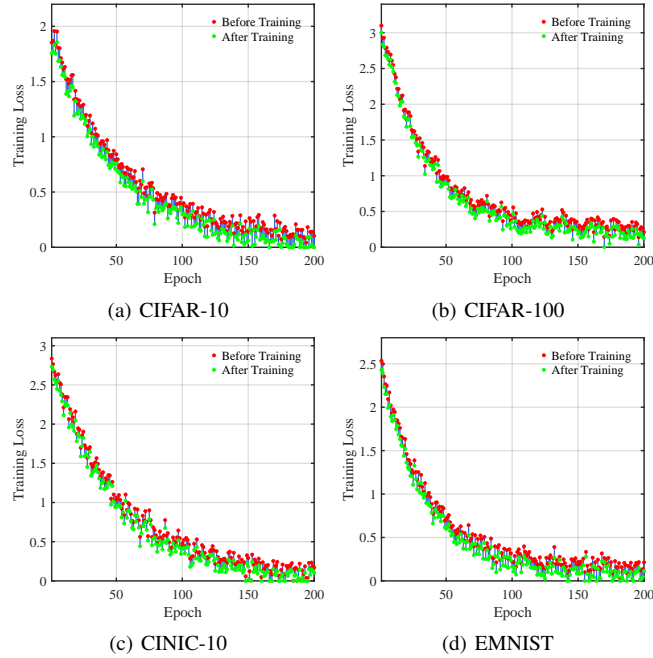


Figure 3. Training loss curves under different dataset.

System communication cost. We conduct a comprehensive evaluation of communication overhead across baseline methods using identical training rounds. As presented in Tab. 1, while lightweight approaches (FedProto, LG-FedAvg, FedPer, and FedRep) incur lower transmission costs compared to conventional FL, their performance remains constrained to specific heterogeneous scenarios. Notably, our method maintains the communication footprint of model-only transmission while achieving competitive accuracy comparable to information-rich alternatives.

Table 1. System communication cost comparison.

Method	Transmission
FedProto	Prototype
LG-FedAvg	Classifier
FedPer	Feature Extractor
FedRep	Feature Extractor
FedBABU	Feature Extractor
FT-FedAvg	Model
MOON	Model
FedFA	Model+Prototype
FedPAC	Model+Prototype
Ours	Equivalent to Model

Hyperparameter analysis. Our framework introduces two key hyperparameters: 1) λ_e for local feature extractor training and 2) λ_c for local classifier adaptation. We systematically evaluate our approach on the CINIC-10 dataset ($s = 70$) with uniform test distribution. Tabs. 2 and 3 demonstrate that extreme values in either direction—excessive or insufficient reliance on global knowledge—respectively cause overfitting or underfitting. The optimal balance emerges at $\lambda_e = 0.8$ and $\lambda_c = 0.6$.

	0.0	0.2	0.5	0.8
Accuracy	47.57	48.62	49.85	50.27
λ_e	1.0	2.0	5.0	7.0
Accuracy	49.94	48.12	43.56	40.29

Table 2. Test accuracy under different values of λ_e .

	0.0	0.2	0.4	0.6
Accuracy	45.68	46.77	48.28	49.97
λ_c	0.8	1.0	2.0	3.0
Accuracy	49.21	48.98	46.38	44.50

Table 3. Test accuracy under different values of λ_c .

Client computational efficiency analysis. We measure overhead by the wall-clock time to reach 70% accuracy on CINIC-10 (Pathology). Our method requires only 17.7 minutes, compared to 18.7–25.3 minutes for baselines; relative to the median baseline (20.85 minutes), this represents a 3.15-minute (15%) speedup. While the feature extractor and classifier are decoupled during local training, consistency between global prototypes and class-level knowledge aligns their objectives, enabling faster convergence with balanced generalization and personalization. The additional discriminator is a lightweight binary classifier, incurring only modest overhead.

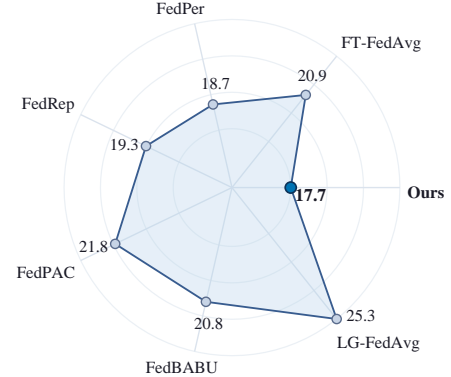


Figure 4. Client computation overhead (minutes).

Single component ablation analysis. To assess the contribution of each component, we conduct ablation studies by isolating them individually (Tab. 2). The results demonstrate that all components provide consistent performance improvements, further underscoring their effectiveness. Moreover, by cross-referencing with Tab. 1 in the main text, we observe that components related to feature extraction and classification decision exhibit strong synergy when combined. In addition, when both feature-level and classifier-level optimization are applied simultaneously, they complement each other and further enhance the consistency optimization process.

Table 4. Single component ablation ($s = 70$).

Method	CINIC-10	CIFAR-10	EMNIST
Backbone	34.73 ± 0.2	54.20 ± 0.1	55.37 ± 0.1
CFT	42.13 ± 0.2	59.67 ± 0.2	63.00 ± 0.2
MPS	40.19 ± 0.2	64.37 ± 0.1	63.57 ± 0.1
CCI	37.55 ± 0.1	61.33 ± 0.1	62.67 ± 0.1
CCF	41.76 ± 0.2	63.89 ± 0.1	64.53 ± 0.1
FedMate	50.24 ± 0.1	72.10 ± 0.1	71.98 ± 0.1

Additional semantic segmentation results. We extend our evaluation to large-scale semantic segmentation using the Cityscapes dataset under extreme heterogeneity conditions (152 clients). Fig. 5 presents qualitative comparisons showing our prototype-recalibration approach consistently outperforms baseline methods in two key aspects: 1) superior visual coherence in predicted segmentation maps, and 2) more precise retention of structural boundaries. These results validate the operational efficacy of our global prototype recalibration mechanism in challenging FL environments.

In addition, we evaluate our method on the PatternNet dataset, which consists of high-resolution remote sensing imagery. The results (Fig. 6) show that our approach yields more fine-grained segmentation, particularly for small or structurally complex categories such as cars, ships, and roads, thereby further demonstrating its robustness across diverse domains and data characteristics.

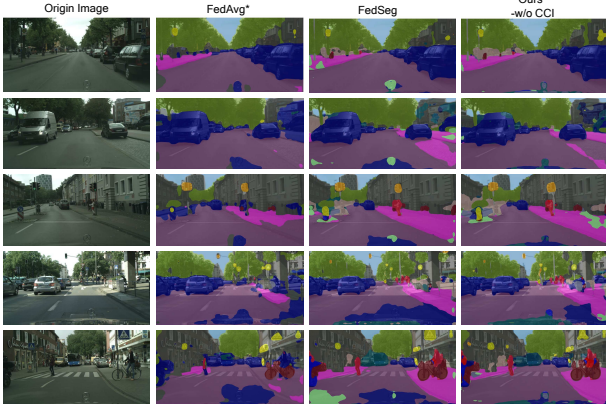


Figure 5. Semantic segmentation results on Cityscapes.

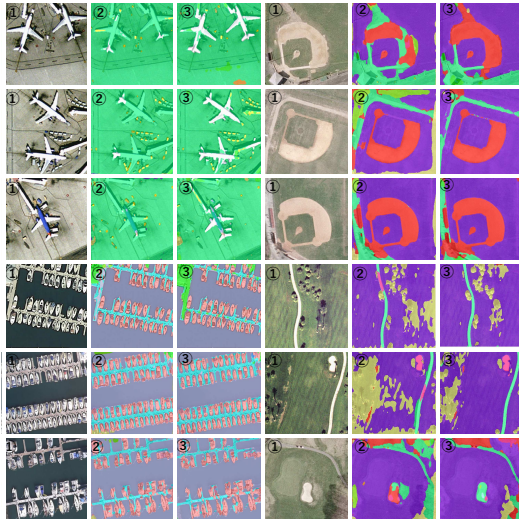


Figure 6. Segmentation on PatternNet: ① Original; ② FedSeg; ③ FedMate.

3 Additional Functional Details

Effectiveness on segmentation tasks. Segmentation can be regarded as a fine-grained extension of classification, where the goal is to perform pixel-level labeling. The success of both classification and segmentation relies on a high-quality feature space, in which intra-class samples are compact while inter-class samples are well separated. Constructing such a feature space requires feature extractors that balance generalization with discrimination. Our method addresses this by incorporating multi-view perspectives, leading to fairer and more robust feature aggregation and yielding an unbiased global prototype. This prototype constrains local feature extractors during training, thereby enhancing the overall feature space. As a result, our approach provides a solid foundation for downstream tasks, including classification, segmentation, and object detection.

Workflow of the CCF module. The CCF component employs two discriminators: a prototype discriminator $D_{pr,i}$ and a classification discriminator $D_{cl,i}$. The prototype discriminator takes local and global prototypes as input through the local classifier ϕ_i and is trained to classify local outputs as 0, while ϕ_i is optimized to produce outputs classified as 1, forming an adversarial process. Similarly, the classification discriminator $D_{cl,i}$ receives the global prototype through both local ϕ_i and global classifiers, distinguishing ϕ_i 's outputs as 0 while forcing ϕ_i to generate outputs closer to 1. To mitigate forgetting, local prototypes are also used to construct a cross-entropy loss. By integrating adversarial learning with prototype supervision, the objective reduces class-specific bias, improves generalization, and alleviates catastrophic forgetting, thereby promoting stronger synergy among complementary knowledge.